

## The Second CIRP Conference on Biomanufacturing

## Design of Highly Porous Hydroxyapatite Scaffolds by Conversion of 3D Printed Gypsum Structures – a Comparison Study

Alan C.S Dantas<sup>a\*</sup>, Debora H. Scalabrin<sup>b</sup>, Roberta De Farias<sup>b</sup>, Amanda A. Barbosa<sup>a</sup>, Andrea V. Ferraz<sup>a</sup>, Cynthia Wirth<sup>c</sup>

<sup>a</sup>Federal University Vale do São Francisco, Av. Antonio Carlos Magalhães 310, Juazeiro-BA, 48902-300, Brazil

<sup>b</sup>Federal University Santa Catarina, Campus Universitário, Florianópolis – SC, 88040-900, Brazil

<sup>c</sup>BAM Federal Institute for Materials Research and Testing, Unter den Eichen 87, 12200 Berlin, Germany

\* Corresponding author. Tel.: +55 74 2102 7633; fax: +55 74 2102 7633. E-mail address: [alan.dantas@univasf.edu.br](mailto:alan.dantas@univasf.edu.br)

### Abstract

Hydroxyapatite (HA) is a bioceramic material with excellent biological properties. However, these properties are strongly dependent of its crystallinity degree, with high values of crystallinity associated to poor resorption rates and bioactivity. This work evaluates the properties of HA samples produced by two different free-forming conformation methods, CNC machining and 3D printing. In both cases, porous gypsum samples were produced and subsequently converted into HA in a reaction with di-ammonium hydrogen phosphate at 100°C and pH 8. A total conversion of the samples was achieved after 36 h independently of the conformation method used. The microstructure, however, before and after the conversion is showed to be dependent on the method used. After conversion the machined samples achieved a maximum compressive strength of 3.5 MPa for porosities of circa 80%, while 3D printed samples achieved a tensile strength of 2.0 MPa by porosities of 61%.

© 2015 The Authors. Published by Elsevier B.V. This is an open access article under the CC BY-NC-ND license (<http://creativecommons.org/licenses/by-nc-nd/4.0/>).

Peer-review under responsibility of the scientific committee of The Second CIRP Conference on Biomanufacturing

**Keywords:** Hydroxyapatite; gypsum; 3D printing; CNC machining

### 1. Introduction

The Araripe region is a mountain range located on the northeast region of Brazil. This region is the greatest producer of gypsite in Brazil and responsible for 89% of all gypsite extracted from the country [1]. The purity of the sources located on this region is of ca 98%. However a great part of this amount is sold without processing or only after basic processing. Such unprocessed material with high purity is sold for a less than US\$ 20/ton. Great part of the industries located in this region works with very basic conditioning methods, such as calcination, which does not necessarily aggregate value to the raw material (ca US\$ 200.00/ton). Alternatively, the raw material has been used in the production of blocks for civil building (US\$ 400/ton) [1].

In this context, the development of new products and processing routes which could increase the added value and improve the commercial potential of the high purity gypsum

extracted from Araripe region is an important way to promote the economic and social development of the region.

Hydroxyapatite (HA) is a biomaterial widely used for the preparation of substitute bone implants. Among the properties of HA are noteworthy the bioactivity, the osseointegration and the similarity with the inorganic phase of the human bone, especially in the form of carbonated HA [2]. Many works have evaluated the mechanical properties of HA in order to produce porous scaffolds with enough mechanical strength to support the loads that acts during the first hours and days of the healing process. Porous HA scaffolds are only recommended to non load bearing applications. However the presence of pores on the scaffolds enhance the cell fixation and the growth of living tissue and blood vessels into the implant creating a strong interface between bone and implant with consequent improvement of the bone regeneration [3].

The production porous HA scaffolds from high purity gypsum bodies shows an interesting method to produce

HA scaffolds with low crystallinity, similar as in human body, where the HA is crystallized at 37°C. The temperatures used in the thermal-bath conversion are reported to be between 100 and 120°C without need for a subsequent heat treatment [4,5].

Additive manufacturing (AM) technologies allow the fabrication of scaffolds in shapes matching the ones of the patient's bone defect, by a direct conversion of a digital data into a 3D model. Among available AM processes, the powder-bed 3D-Printing operates with the successive addition of powdery material, layer-upon-layer, to form the final 3D model. The process allows, in this way, a better control of pore sizes, pore morphology and porosity of the matrix, if compared with other fabrication methods [6,7,8]. Studies have proved that layer thickness and binder saturation have a significant effect on the strength, integrity, and dimensional accuracy of 3D printed samples [9]. Recently, structures similar to the actual trabecular bone structure have been produced via 3D printing and characterized [10,11].

The aim of this work is a comparison of two different methods to produce form free scaffolds by conversion of high purity gypsum into HA. The bodies were produced via machining of gypsum blocs using a CNC device and via 3D printing of porous bodies from gypsum powder. After forming, the bodies were converted into HA. The structural and mechanical properties of the samples have been evaluated and compared before and after conversion into HA.

## 2. Materials and Methods

### 2.1. Preparation of Gypsum Structures by CNC machining

B-Gypsum (calcium sulfate hemihydrate,  $\text{CaSO}_4 \cdot 0.5\text{H}_2\text{O}$ , 95% of purity, Gesso Mineral AG) and PVA (99% hydrolyzed, Sigma-Aldrich, USA) have been mixed using different proportions of polymer (0, 1, 5, 10 and 15 wt.%). Gypsum/PVA slurries have been prepared using water/solid mass ratio of 0.7. Porous bodies were prepared by casting of the slurry in molds. Gypsum/PVA bodies were machined in a CNC lathe (Nardini, MS.220.G F2 KJL 919) using Solid Works based CAD models. After machining the gypsum/PVA bodies were immersed in water for approximately 2 hours, at a temperature of 90°C, in order to extract the polymer from the ceramic bodies.

### 2.2. Production of 3D printed gypsum structures

Gypsum hemihydrate powder with an average particle size of 10  $\mu\text{m}$  was produced via calcination of high purity gypsum rocks at 180°C for 4 hours. The gyps site was provided from Araripe region located in Brazil. After calcination, the powder presented a Hausner ratio of 1.65, indicative of poor flowability. The powder has been printed in a Prometal R1 (ExOne, USA), operating with a vacuum device for stabilization of the power bed [12]. Double distilled water containing 1 vol-% binder (Aqueous-Based Binder, ExOne, USA) was used to regulate the surface stress of the water particles during the printing process. After printing the samples were cleaned and subsequently immersed in water to ensure a complete dihydrate formation.

### 2.3. Conversion of gypsum into HA

The structures were submersed in 200 mL of  $(\text{NH}_4)_2\text{HPO}_4$  0.5  $\text{mol.L}^{-1}$  solution in a three-neck flask at a temperature of 100°C for 36 hours. The pH of the medium was controlled by adding  $\text{NH}_4\text{OH}$  6.0  $\text{mol.L}^{-1}$  solution. At the end of the reaction time, the blocks were washed in de-ionized water until reaching neutral pH and then dried in an oven at 50°C for approximately 4 hours.

### 2.4. Characterization

The samples before and after conversion were characterized by X-ray diffraction (XRD) (Diffract ACT series 1000 SIEMENS, radiation  $\text{Cu-K}\alpha$ ) and Scanning Electron Microscopy (SEM) ZEISS Gemini Supra 40 equipped with a EDS Bruker Quantax 400. Compressive strength of the machined samples ( $\sigma_c$ ) were carried out using a Universal Mechanical Testing Machine (EMIC-DL 10000) in cylindrical samples of  $\phi$  11 mm x 22 mm. Mechanical strength of 3D printed samples was carried out in a universal mechanical test machine (Z005, Zwick/Roell) using the four spheres method.

## 3. Results

### 3.1. Machined gypsum bodies and conversion into HA

Fig. 1A shows the fracture surface of a gypsum structure without addition of binder. The microstructure consists of crystals in prismatic needle shape. The EDS analysis confirmed the high purity of the gypsum where only Ca and S peaks were observed.

The addition of PVA promoted a homogeneous distribution of the polymer resulting in a reinforcement of the samples, followed by a slight change in the size and form of the crystals. Due to the hydrophilic nature of PVA a larger interaction between the polymer and the hydration water was promoted. Consequently the crystals show better adherence to the PVA grains, causing greater interaction between crystals and polymer particles [1]. Macroscopically, the addition of PVA promoted an increase in the mechanical properties and the machining of the samples became possible. A minimum addition of 15%-mass PVA was necessary to permit the machining of the samples. Before the conversion into HA the amount of PVA was removed to prevent a negative interference of the PVA on the conversion process.

Fig. 1B shows the fracture surface of the samples after conversion HA for 36 hours. A great change on the morphology can be observed on the surface of the samples, in comparison to the gypsum morphology showed in Fig 1A. After conversion the surface presents particles of circular shape and a high porosity can be observed. The EDS analysis obtained for this sample confirmed the presence of the chemical elements Ca and P, which are characteristic for HA.

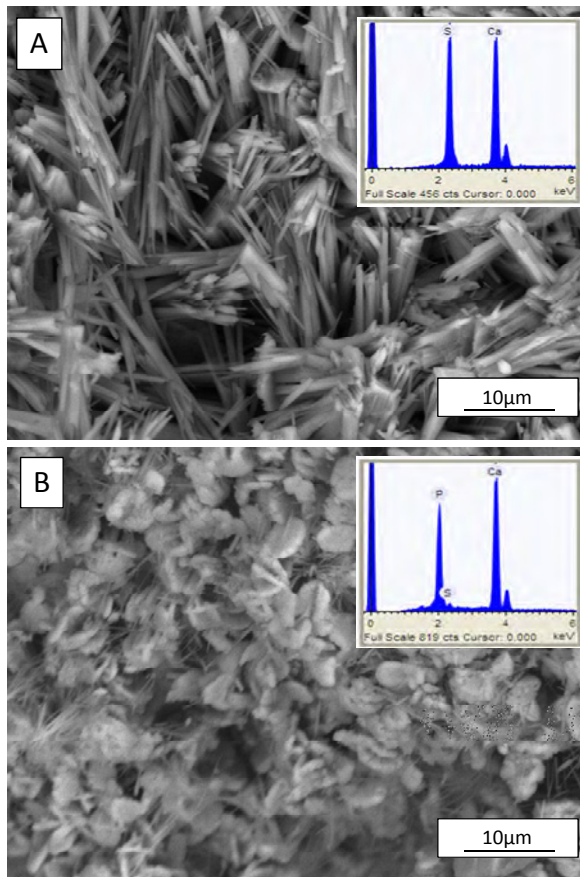


Fig. 1. (a) Fracture surface of pure gypsum after hardening and (b) Fracture surface of a HA sample produced by conversion of gypsum for 36 hours.

The XRD patterns of the samples before and after conversion are showed in Fig. 2, where a total conversion of the Gypsum in HA can be verified after 36 hours of reaction. Lower reaction times lead to an incomplete conversion of gypsum into HA. The maximum intensities peaks of gypsum at  $2\theta = 11.63^\circ$  and  $20.7^\circ$  were not present on the patterns of the samples after conversion.

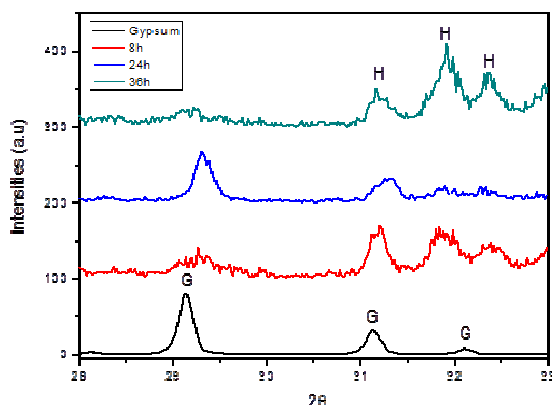


Fig. 2. XRD Patterns of the machined samples before and after conversion for 8h, 24h and 36h.

After removal of the PVA formation of pores was observed. The total amount of pores presents on these samples increased, and a reduction of the mechanical properties was promoted. The samples with 15 %-masse of binder showed a geometrical porosity of  $43 \pm 0.2\%$ , smaller than that reached for gypsum without PVA ( $56 \pm 2\%$ ). However after removal of the binder the geometrical porosity reached a value of  $68 \pm 1.5\%$ .

An increase of the compressive strength was observed by increase of the PVA amount. Samples with 15 %-masse PVA reached a maximum strength of  $13.5 \pm 0.45$  MPa, while samples produced without binder reached a maximum compressive strength of  $9.2 \pm 0.4$  MPa. After removal of the binder the compressive strength of the samples was reduced to a value similar to the sample produced without binder,  $10.4 \pm 0.3$  MPa.

After 36 hours conversion, the compressive strength ( $\sigma_c$ ) reached a maximum of  $3.5 \pm 0.1$  MPa for a porosity of  $80 \pm 0.9\%$ . Comparing to the samples before conversion, that reached a  $\sigma_c$  of  $10.4 \pm 0.3$  MPa and a final geometrical porosity of  $68 \pm 1.5\%$ , it can be seen that the conversion of gypsum in HA promotes an additional increase of the porosity probably related to the change on crystal morphology, as seen in Fig. 5. However the samples still reached 3.5 MPa, which is enough to handling of the samples. The CAD models used to machining the samples and the form of the machined samples can be seen in Fig. 3.

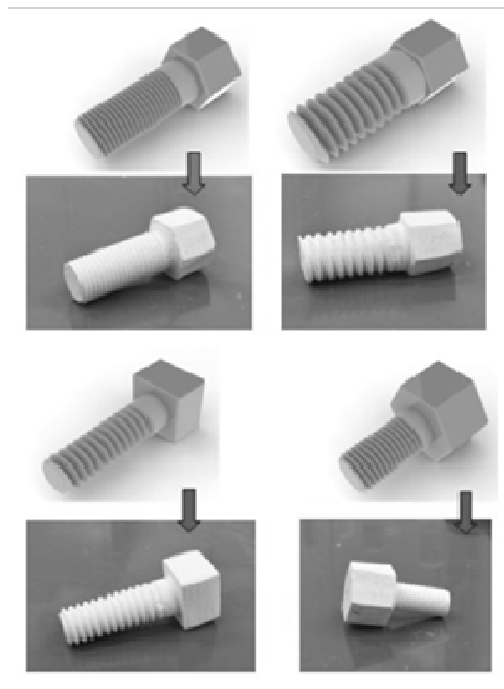


Fig. 3. CAD Modeling and machined screws produced with gypsum bodies reinforced with 15% PVA.

### 3.2. 3D printed gypsum structures and conversion in HA

The morphology of 3D printed fracture surfaces can be seen in Fig 4A, where the peculiar shape of the dehydrate crystals can be observed. EDS of the samples presents only Ca, S and O peaks related to the calcium sulphate. Fig 4B shows the surface morphology of the sample after conversion for 36 hours, with round morphology of the HA crystals. EDS patterns confirmed a total conversion of the samples into HA, where only peaks related to Ca, P and O can be observed. These crystals consisted of great agglomerates formed by particles with an average particle size of 0.5  $\mu\text{m}$ .

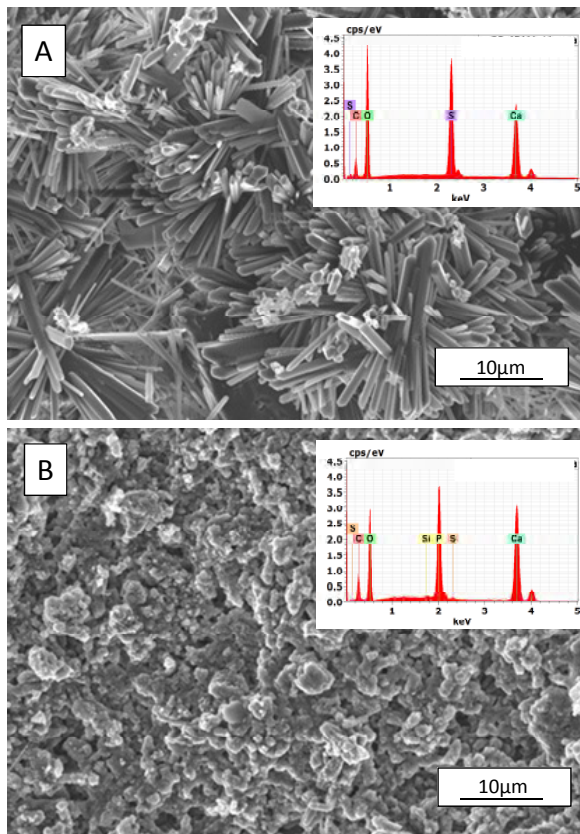


Fig. 4. (a) Surface morphology of 3D printed gypsum samples and (b) surface morphology of the HA converted samples.

Comparing the starting morphologies of the gypsum crystals present in cast and 3D printed parts (Fig. 1A and 4A, respectively), it is possible to note that the gypsum crystals on 3D printed parts present a different morphology in comparison with the cast samples. Cast samples were prepared by mixing the gypsum with PVA. In turn, the samples have crystallized in presence of PVA, showing then a higher needle aspect with very thin crystals. The 3D printed samples have shown wider crystals and were produced without presence of binder. After conversion the samples also showed differences on the surface morphology in comparison with the machined samples, probably due to the different gypsum start crystals.

Also for 3D printed parts, the conversion into HA was only completed after 36 hours of reaction. Fig. 5 shows the XRD patterns of the samples after different conversion times. After 8 hours the HA peaks located at  $2\theta = 31.7^\circ$  and  $32.2^\circ$  can be observed. However a complete conversion without traces of calcium sulfate was only observed after 36h.

The formed HA peaks presents low intensity and broad shape, which is related to small crystallite sizes. Tadic and Epple [2] performed the XRD of different types of human bone and related the small crystallite size as a characteristic from natural bone. The low crystallite size enhance the solubility of the HA that become bioresorbable like natural bone.

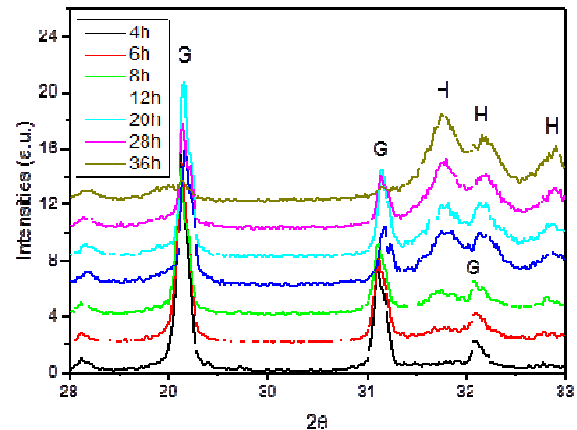


Fig. 5. XRD Patterns of the 3D printed samples after conversion at different times.

The porosity of printed samples achieved prior and after conversion have been determined,  $58 \pm 3\%$  and  $61 \pm 3\%$ , respectively. The bending strength has been measured of circa  $3.5 \pm 0.6$  MPa (prior conversion) and  $2.0 \pm 0.3$  MPa (after conversion). The lost of the mechanical properties can be related to the change on the crystal form once the gypsum presents long crystals that form an interconnected net able to transfer the load across the crystals. However the samples HA samples still presents good mechanical stability.

Fig. 6 shows the samples produced on this work where a good dimensional precision can be observed. The geometrical density of the samples was of  $0.75 \pm 0.02$  g/cm<sup>3</sup>, that is related to a porosity of  $74.3 \pm 0.8\%$ .



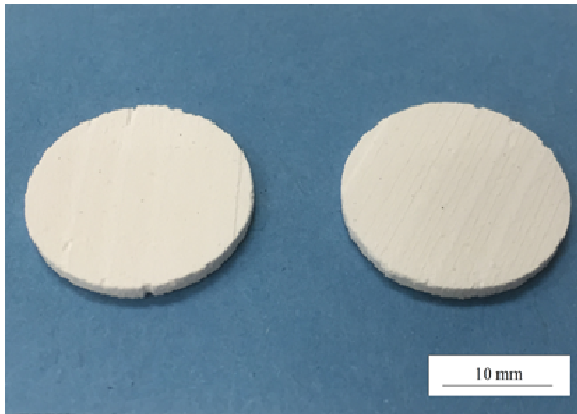


Fig. 6. Samples produced by 3D printing of granulated gypsum.

#### 4. Discussion

##### 4.1. Conversion of gypsum into HA

The results showed that independent of the method and the porosity of the samples the conversion of gypsum into HA was only reached after 36 hours of reaction. This indicates that the conversion mechanism is independent of the porosity and consequently of the surface area available to reacts. Other interesting result is related to the shape of HA crystals that are formed after conversion. The crystals formed in the machined samples present a different morphology more spherical than for the crystals formed in the 3D printed samples. In these samples the crystals presented a rough morphology formed by agglomerates of particles of some nanometers.

The gypsum produced by casting with PVA present a slightly difference in morphology, if compared with the 3D printed samples. The differences are mainly due to the presence of PVA that inhibits the crystal growth of the gypsum crystals [4]. Thus the crystals present the shape of thin needles, while the 3D crystals presents more wide. The printing process of the powder used a saturation of 300% that means a water amount of 3 Times for each amount of gypsum. So these samples were produced with a water/gypsum (W/G) ratio of 1.5 while the casted samples were produced with a W/G ratio of 0.7.

##### 4.2. Advantages and disadvantages of each method

The methods presented on this work are both interesting to achieve low crystalline HA porous bodies however each have different particularities. The table 1 show the principal characteristics of the methods related to different evaluation fields.

Table 1. Different properties of the samples produced by 3D printing and CNC machining

Property	CNC machining	3D printing
Sample preparation	Need a minimum of 15% Binder	Particle sizes > 15µm
Preparation time	Casting, drying,	Printing, drying,

	machining, extraction of binder, conversion.	conversion
Free freedom	Limited by machining	Limited by process accuracy
Porosity	Between 50 and 80 %	Between 50 and 80%
Mechanical strength	Maximum $\sigma_c$ of $3.5 \pm 0.1$ for a porosity of 80 %	Maximum $\sigma_c$ of $2.0 \pm 0.3$ for a porosity of 61%

Gypsum blocs need a minimum of 15 masse-% polymeric binder in order to produce blocs with enough mechanical properties and able to be machined. This binder must be extracted from the samples before conversion leading to a increase in the preparation time. The preparation of the 3D printed samples however needs strategies to stabilize the powder bed. Gypsum powder presents normally average particle size under the optimized printable value of 45µm and 100µm. So is necessary a granulation with a polymeric binder or the utilization of a vacuum device to stabilize the powder bed. The second alternative is very useful, because avoid a additional step for binder extraction.

Depending on the amount of binder the machined samples can achieve higher densities above 80 %. However the utilization of binder amounts above 15 % lead to a strong decrease on the mechanical strength [5]. For the 3D printed samples, the porosity depends on the saturation applied and can reach values of 75%, however with lower mechanical properties.

#### 5. Conclusion

The preliminary studies of 3D printed gypsum structures for subsequent conversion in HA show many advantages in comparison with the machining of slip cast structures. One of the most important is the form freedom, once many details impossible or very hard to be machined can be produced by 3D printing. Others are related to the no-need of higher binder contents, in comparison to the minimum of 15% used to produce machinable structures. The shortening in the processing chain from 2:1 CNC-machining: 3D-printing turn the technology economically attractive for the process of low-cost raw materials. However additional work must be done in order to improve the mechanical properties of the samples by adjustment of the printing parameters.

#### Acknowledgements

The authors acknowledge the CAPES for financial support under the “Science without borders Program”, process number 248861/2013-1.

#### References

- [1] Lyra Sobrino, A.C.P., Amaral, A.J.R., Dantas J.O.C., (Gypsite, Gipsita, Report of the Brazilian department of mineral production - DNPM, Salvador Brazil, 2009
- [2] Tadic, D., Eppe, M. A thorough physicochemical characterisation of 14 calcium phosphate-based bone substitution materials in comparison to natural bone, *Biomaterials* 25 (2004) 987–994

- [3] Wintermantel, E., Ha S.W., *Biokompatible Werkstoffe und Bauweisen: Implantaten für Medizin und Umwelt*, Springer, Berlin-Heidelberg, 1996
- [4] Furuta, S., Katsuki, H., Komarneni, S., Porous hydroxyapatite monoliths from gypsum waste. *J. Mater. Chem.* 8, 2803-2806, 1998.
- [5] Barbosa, A. A.; Ferraz, A. V.; Olivier, N. C.; Dantas, A. C. S. The Production of Hydroxyapatite Prototypes from Solid Bodies of Gypsum/Poliviny Alcohol Composites. *Materials Research*, vol. 17, p. 39-44, 2014.
- [6] Hollister, S.J., Porous scaffold design for tissue engineering. *Nat Mater* 4(7), 518-524, 2005.
- [7] Wu, C., Luo, Y., Cuniberti, G., Xiao, Y., and Gelinsky, M. Three-dimensional printing of hierarchical and tough mesoporous bioactive glass scaffolds with a controllable pore architecture, excellent mechanical strength and mineralizationability. *Acta Biomater* 7, 2644, 2011.
- [8] Loh Q. L., and Choong C., Three-Dimensional Scaffolds for Tissue Engineering Applications: Role of Porosity and Pore Size *TISSUE ENGINEERING: Part B Volume 19, (6)*, 2013
- [9] Vaezi, M., Chua, C.K., Effects of layer thickness and binder saturation level parameters on 3D printing process *Int J Adv Manuf Technol* (2011) 53:275–284
- [10] Podshivalov, L., Gomes, C.M., Zocca, A., Guenster, J., Bar-Yoseph, P., Fischer, A., Design, analysis and additive manufacturing of porous structures for biocompatible micro-scale scaffolds. *Procedia CIRP*, 5 p. 247 – 252, 2013 (doi: 10.1016/j.procir.2013.01.049)
- [11] Gomes, C.M., Podshivalov, L., Zocca, A., Guenster, J., Bar-Yoseph, P., Fischer, A., Designing apatite/wollastonite (A/W) porous scaffolds by powder-based 3D printing, in: *High Value Manufacturing: Advanced Research in Virtual and Rapid Prototyping: Proceedings of the 6th International Conference on Advanced Research in Virtual and Rapid Prototyping*, Leiria, Portugal, 1-5 October, 2013.
- [12] Günster, J., Zocca, A., Gomes Morais, C., *Verfahren zum Auftrag von Pulverschichten mittels Gasstrom für die additive Fertigung*, DE 102014109706, 2014.